

A general framework for Vecchia approximations of Gaussian processes

Matthias Katzfuss* Joseph Guinness†

Abstract

Gaussian processes (GPs) are commonly used as models for functions, time series, and spatial fields, but they are computationally infeasible for large datasets. Focusing on the typical setting of modeling observations as a GP plus an additive noise term, we propose a generalization of the Vecchia (1988) approach as a framework for GP approximations. We show that our general Vecchia approach contains many popular existing GP approximations as special cases, allowing for comparisons among the different methods within a unified framework. Representing the models by directed acyclic graphs, we determine the sparsity of the matrices necessary for inference, which leads to new insights regarding the computational properties. Based on these results, we propose a novel sparse general Vecchia approximation, which ensures computational feasibility for large datasets but can lead to tremendous improvements in approximation accuracy over Vecchia’s original approach. We provide several theoretical results, conduct numerical comparisons, and apply the methods to satellite data. We conclude with guidelines for the use of Vecchia approximations.

Keywords

covariance approximation; directed acyclic graphs; large datasets; computational complexity; sparsity; spatial statistics

1 Introduction

Gaussian processes (GPs) have become popular choices as models or prior distributions for functions, time series, and spatial fields (e.g., Banerjee et al., 2004; Rasmussen and Williams, 2006; Cressie and Wikle, 2011). The defining feature of a GP is that the joint distribution of a finite number of observations is multivariate normal. However, since computing with multivariate normal distributions incurs quadratic memory and cubic time complexity in the number of observations, GP inference is generally infeasible when the data size is in the tens of thousands or higher, limiting the direct use of GPs for many of the large datasets available today.

*Department of Statistics, Texas A&M University. katzfuss@gmail.com

†Department of Statistics, North Carolina State University. jsguinne@ncsu.edu

To achieve computational feasibility, numerous approaches have been proposed in the statistics and machine-learning literatures. These include approaches leading to sparse covariance matrices (Furrer et al., 2006; Kaufman et al., 2008), sparse inverse covariance (i.e., precision) matrices (Rue and Held, 2005; Lindgren et al., 2011; Nychka et al., 2015), and low-rank matrices (e.g., Higdon, 1998; Wikle and Cressie, 1999; Quiñonero-Candela and Rasmussen, 2005; Banerjee et al., 2008; Cressie and Johannesson, 2008; Katzfuss and Cressie, 2011). Several other approaches are described in Section 2.4.

In this article, we extend and study Vecchia’s approach (Vecchia, 1988), one of the earliest proposed GP approximations, which leads to a sparse Cholesky factor of the precision matrix. Based on some ordering of the GP observations, Vecchia’s approximation replaces the high-dimensional joint distribution with a product of univariate conditional distributions, in which each conditional distribution only conditions on a small subset of previous observations in the ordering. This approximation incurs low computational and memory burden, it has been shown to be highly accurate in terms of Kullback-Leibler divergence from the true model (e.g., Guinness, 2016), and it is amenable to parallel computing because each term can be computed separately.

We consider the typical setting of observations from a GP that include an additive noise or nugget component. Datta et al. (2016a) proposed to apply Vecchia’s approximation to the latent GP instead of the noisy observations, but Finley et al. (2017) noted that this approach “require[d] an excessively long run time.” Here, we propose a generalized version of the Vecchia approximation, which allows conditioning on both latent and observed variables. We show that our general Vecchia approach contains several popular state-of-the-art GP approximations as special cases, allowing for comparisons among the different approaches within a unified framework. We give computationally efficient formulas for computing likelihoods and predictions in the presence of noise. Further, we describe how approximations within the general Vecchia framework can be represented by directed acyclic graph (DAG) models, and we use the connection to DAGs to prove results about the sparsity of the matrices appearing in the inference algorithms. The results lead to new insights regarding computational properties, including shedding light on the computational problems with latent Vecchia noted in Finley et al. (2017). Based on these results, we propose a particular instance of the general Vecchia framework, which we call sparse general Vecchia (SGV), that comes with guaranteed levels of sparsity in its matrix representation but can lead to tremendous improvements in approximation accuracy over Vecchia’s original approach. In addition to the theoretical results, we provide numerical studies exploring different options within the general Vecchia framework and comparing our novel SGV to existing approximations. We will freely supply all of our code upon publication.

This article is organized as follows. In Section 2, we review Vecchia’s approximation, introduce our general Vecchia framework, describe several existing GP approximations as special cases, and detail connections to DAGs. In Section 3, we consider inference within the framework, including introducing the necessary matrices and studying their sparsity, and deriving the computational complexity. In Section 4, we describe our new SGV approximation and contrast it with two existing approaches. Section 5 contains additional insights on ordering and conditioning. Numerical results and comparisons can be found in Section 6, and an application to satellite data is given in Section 7. In Section 8, we conclude and provide guidelines for the use of Vecchia approximations. All proofs can be found in Appendix A.

2 A general Vecchia approach

2.1 Noisy observations of a Gaussian process

Let $\{y(\mathbf{s}) : \mathbf{s} \in \mathcal{D}\}$, or $y(\cdot)$, be the true process of interest on a continuous (i.e., non-gridded) domain $\mathcal{D} \subset \mathbb{R}^d$, $d \in \mathbb{N}^+$. We assume that $y(\cdot) \sim GP(0, K)$ is a zero-mean Gaussian process (GP) with covariance function $K : \mathcal{D} \times \mathcal{D} \rightarrow \mathbb{R}$. We place no restrictions on K , other than assuming that it is a positive-definite function that is known up to a vector of parameters, $\boldsymbol{\theta}$. Usually, K will be a continuous covariance function without a nugget component (which will be added in the next paragraph). In most applications, $y(\cdot)$ will not have zero mean, but estimating and subtracting the mean is typically not a computational problem, so we ignore the mean here for simplicity. Further, let $\mathcal{S} \subset \mathcal{D}$ be some finite set of locations in the domain \mathcal{D} , partitioned as $\mathcal{S} = \{\mathcal{S}_1, \dots, \mathcal{S}_\ell\}$, where $|\mathcal{S}_i| = r_i$ is the size of \mathcal{S}_i , and define $\mathbf{y} := (\mathbf{y}'_1, \dots, \mathbf{y}'_\ell)'$, where $\mathbf{y}_i := \mathbf{y}(\mathcal{S}_i)$ is the vector obtained by evaluating the GP $y(\cdot)$ at locations \mathcal{S}_i .

We assume that our observations of the GP $y(\cdot)$ include an additive Gaussian noise or nugget term. This assumption is ubiquitous in spatial statistics, GP regression, and functional data, and it has even been proposed for the modeling of computer experiments (Gramacy and Lee, 2012). Specifically, we observe $\mathbf{z} = (\mathbf{z}'_1, \dots, \mathbf{z}'_\ell)'$, distributed as $\mathbf{z}_i | \mathbf{y} \stackrel{ind.}{\sim} \mathcal{N}(\mathbf{O}_i \mathbf{y}_i, \mathbf{R}_i)$, where \mathbf{O}_i is an $r_i^z \times r_i$ observation matrix, and \mathbf{R}_i is assumed to be a positive-definite matrix describing the noise variance. In the simplest case, we have $\mathbf{O}_i = \mathbf{I}_{r_i}$ and $\mathbf{R}_i = \tau^2 \mathbf{I}_{r_i}$, although that is not required. For example, \mathbf{R}_i might not be diagonal, indicating some dependence in the noise term. Or, not all entries of \mathbf{y}_i might be observed, so that \mathbf{O}_i is a submatrix of the identity matrix with $r_i^z < r_i$ (or even $r_i^z = 0$ if none of the entries of \mathbf{y}_i are observed). Parameters $\boldsymbol{\theta}$ in K and \mathbf{R}_i will be assumed to be known for now; parameter inference will be discussed in Section 3.2.

Define $h(i) := \{1, \dots, i-1\}$ to be the “history” of i with $h(1) = \emptyset$, and so $\mathbf{z}_{h(i)} = (\mathbf{z}'_1, \dots, \mathbf{z}'_{i-1})'$. The joint density for the observed variables (i.e., the likelihood) can be written as

$$f(\mathbf{z}) = \prod_{i=1}^{\ell} f(\mathbf{z}_i | \mathbf{z}_{h(i)}). \quad (1)$$

Working with or evaluating the density in (1) directly incurs $O(n_z^2)$ memory and $\mathcal{O}(n_z^3)$ computational cost, and is thus infeasible for large n_z , where n_z is the length of \mathbf{z} .

2.2 Brief review of Vecchia’s approximation

To avoid computational difficulties associated with storing and factoring large covariance matrices, Vecchia’s approximation (Vecchia, 1988; Stein et al., 2004) replaces $h(i)$ with a subset $g(i) \subset h(i)$, where $g(i)$ is usually (but not necessarily) chosen to contain those indices corresponding to observations nearby in distance to the i th vector of observations. We refer to $g(i)$ as the i th conditioning set, and to $\mathbf{z}_{g(i)}$ as the conditioning vector for \mathbf{z}_i . This leads to the (standard) Vecchia approximation of the joint density in (1):

$$\widehat{f}(\mathbf{z}) = \prod_{i=1}^{\ell} f(\mathbf{z}_i | \mathbf{z}_{g(i)}) \quad (2)$$

Cressie and Davidson (1998) showed that this implies a Markov random field model with sparse precision matrix. Stein et al. (2004) showed that maximizing (2) corresponds to solving a set of unbiased estimating equations, and they proposed a residual maximum likelihood (REML) method for estimating covariance parameters.

2.3 The general Vecchia framework

The standard Vecchia approach in Section 2.2 applies to the vector of observations, \mathbf{z} . We propose here a general Vecchia approach, which is a Vecchia approximation applied to the vector $\mathbf{x} = (\mathbf{x}'_1, \dots, \mathbf{x}'_b)'$:= $(\mathbf{y}'_1, \mathbf{z}'_1, \mathbf{y}'_2, \mathbf{z}'_2, \dots, \mathbf{y}'_\ell, \mathbf{z}'_\ell)'$ composed of both latent and observed variables. Here, $\mathbf{x}_{2i-1} = \mathbf{y}_i$, $\mathbf{x}_{2i} = \mathbf{z}_i$, and $b = 2\ell$. More precisely, the general Vecchia approximation is defined as

$$\widehat{f}(\mathbf{x}) = \prod_{i=1}^b f(\mathbf{x}_i | \mathbf{x}_{g(i)}) = \prod_{i=1}^{\ell} f(\mathbf{y}_i | \mathbf{x}_{g(2i-1)}) f(\mathbf{z}_i | \mathbf{x}_{g(2i)}). \quad (3)$$

Since the true model assumes that \mathbf{z}_i is conditionally independent of every other subvector given \mathbf{y}_i , we always choose $g(2i) = \{2i - 1\}$, so that the conditioning vector for $\mathbf{x}_{2i} = \mathbf{z}_i$ is $\mathbf{x}_{g(2i)} = \mathbf{x}_{2i-1} = \mathbf{y}_i$. On the other hand, we allow the conditioning vector for \mathbf{y}_i to be any subvector of $(\mathbf{y}'_1, \mathbf{z}'_1, \dots, \mathbf{y}'_{i-1}, \mathbf{z}'_{i-1})'$. As \mathbf{y}_j can implicitly contain information on $\mathbf{z}_1, \dots, \mathbf{z}_j$, it can be more accurate but also more computationally expensive to condition on \mathbf{y}_j rather than on \mathbf{z}_j ; we will explore this tradeoff in Section 4.

To simplify the notation to follow, we define $p(i) := g(2i - 1)$, and so $\mathbf{x}_{p(i)}$ is the conditioning vector for \mathbf{y}_i . Further, we define $q_y(i) := \{j \in \mathbb{N} : (2j - 1) \in p(i)\}$, $q_z(i) := \{j \in \mathbb{N} : 2j \in p(i)\}$, and their union $q(i) := q_y(i) \cup q_z(i)$ will be referred to as the conditioning index set. Then we have $\mathbf{x}_{p(i)} = (\mathbf{y}'_{q_y(i)}, \mathbf{z}'_{q_z(i)})'$. Stated another way, $j \in q_y(i)$ signifies that \mathbf{y}_i conditions on \mathbf{y}_j , while $j \in q_z(i)$ signifies that \mathbf{y}_i conditions on \mathbf{z}_j instead. Note that, due to conditional independence of \mathbf{y}_i and \mathbf{z}_j given \mathbf{y}_j , there is no point in including both \mathbf{y}_j and \mathbf{z}_j in $\mathbf{x}_{p(i)}$, and so we assume $q_y(i) \cap q_z(i) = \emptyset$. This gives the alternative expression of (3):

$$\widehat{f}(\mathbf{x}) = \prod_{i=1}^{\ell} f(\mathbf{y}_i | \mathbf{x}_{p(i)}) f(\mathbf{z}_i | \mathbf{y}_i) = \prod_{i=1}^{\ell} f(\mathbf{y}_i | \mathbf{y}_{q_y(i)}, \mathbf{z}_{q_z(i)}) f(\mathbf{z}_i | \mathbf{y}_i).$$

Usually, it is of interest to evaluate an approximation to $f(\mathbf{z})$, which involves integrating the approximation for the joint density of \mathbf{z} and \mathbf{y} over the latent vector \mathbf{y} as follows:

$$\widehat{f}(\mathbf{z}) = \int \widehat{f}(\mathbf{x}) d\mathbf{y} = \int \left(\prod_{i=1}^{\ell} f(\mathbf{y}_i | \mathbf{x}_{p(i)}) f(\mathbf{z}_i | \mathbf{y}_i) \right) d\mathbf{y}. \quad (4)$$

If the conditioning sets are equal to the respective history sets (i.e., $p(i) = h(2i - 1)$ for all i), the exact distribution $f(\mathbf{z})$ in (1) is recovered. In this sense, the Vecchia approximations considered here converge to the truth as the conditioning sets grow larger. However, large conditioning sets negate the computational advantages, and thus the case of small conditioning sets is of interest here.

In summary, a general Vecchia approximation $\widehat{f}(\mathbf{x})$ of the multivariate normal distribution $f(\mathbf{x})$, and thus the implied distribution $\widehat{f}(\mathbf{z})$ of a vector of noisy observations \mathbf{z} of a GP $y(\cdot)$, is determined by the following choices:

- C1:** Choose a set of locations \mathcal{S} , which is usually a superset of the observed locations.
- C2:** Choose a partitioning of \mathcal{S} into ℓ subsets.
- C3:** Choose an ordering of the location subsets as $\mathcal{S} = \{\mathcal{S}_1, \dots, \mathcal{S}_\ell\}$.
- C4:** For each $i = 2, \dots, \ell$, choose a conditioning index set $q(i) \subset \{1, \dots, i-1\}$ for \mathbf{y}_i . (We always have $q(1) = \emptyset$.)
- C5:** For each $i = 2, \dots, \ell$, partition $q(i)$ into $q_y(i)$ and $q_z(i)$; that is, for each $j \in q(i)$, choose whether \mathbf{y}_i should condition on \mathbf{y}_j or \mathbf{z}_j .

For C1, the default choice is often to set \mathcal{S} equal to the observed locations, and $\mathbf{O}_i = \mathbf{I}_{r_i}$. A major focus of this article is C5, which is discussed in Section 4. In Section 5, we provide some insights into C2–C4, and in Section 6 we explore C3–C5 numerically.

2.4 Existing methods as special cases

Many existing GP approximations fall into the framework described above. We give some examples here. Most of these examples are illustrated in Figure 1.

2.4.1 Standard Vecchia and extensions

The original approach of this form was proposed in Vecchia (1988) with $r_i = 1$, ordering locations by a spatial coordinate (henceforth referred to as coord ordering), and only conditioning on the nearest observations (as opposed to latent y 's); that is, $q_z(i) = q(i)$ and $q_y(i) = \emptyset$. Using (4), this results in the approximation

$$\hat{f}(\mathbf{z}) = \int \left(\prod_{i=1}^{\ell} f(\mathbf{z}_i | \mathbf{y}_i) f(\mathbf{y}_i | \mathbf{z}_{q(i)}) \right) d\mathbf{y} = \prod_{i=1}^{\ell} \int f(\mathbf{z}_i | \mathbf{y}_i, \mathbf{z}_{q(i)}) f(\mathbf{y}_i | \mathbf{z}_{q(i)}) d\mathbf{y}_i = \prod_{i=1}^{\ell} f(\mathbf{z}_i | \mathbf{z}_{q(i)}),$$

where $f(\mathbf{z}_i | \mathbf{y}_i) = f(\mathbf{z}_i | \mathbf{y}_i, \mathbf{z}_{q(i)})$ because \mathbf{z}_i is conditionally independent of $\mathbf{z}_{q(i)}$ given \mathbf{y}_i under the true model. Stein et al. (2004) recommended to include in $q(i)$ the indices of some close and some far-away observations, and grouping observations (i.e., $r_i > 1$) for computational advantages. Guinness (2016) considered an adaptive grouping scheme, and discovered that ordering schemes other than coord ordering can drastically improve approximation accuracy. Vecchia (1988) and Stein et al. (2004) focus on likelihood approximation, but Guinness (2016) also considers spatial prediction via conditional simulation. Further extensions were proposed in Sun and Stein (2016) and Huang and Sun (2016).

2.4.2 Nearest-neighbor GP (NNGP)

The NNGP (Datta et al., 2016a,b,c) considers explicit data models (such as the additive Gaussian noise assumed here), and conditions only on latent variables: $q_y(i) = q(i)$ and $q_z(i) = \emptyset$. A GP is defined by setting $r_i \equiv 1$ and splitting $\mathcal{S} = \{\mathcal{Q}, \mathcal{T}\}$ into a fixed set of “knot” locations \mathcal{Q} (often unobserved), and the remaining locations \mathcal{T} . Based on a coord ordering of \mathcal{Q} , nearest-neighbor conditioning is used, with the constraint that variables at locations \mathcal{T} can only condition on those in \mathcal{Q} ; that is, if $|\mathcal{Q}| = n_{\mathcal{Q}}$, then $q(i) \subset \{1, \dots, n_{\mathcal{Q}}\}$ for any $i > n_{\mathcal{Q}}$.

2.4.3 Independent blocks

The simplest special case is given by empty conditioning sets $p(i) = \emptyset$ for every i :

$$\widehat{f}(\mathbf{z}) = \int \left(\prod_{i=1}^{\ell} f(\mathbf{z}_i | \mathbf{y}_i) f(\mathbf{y}_i) \right) d\mathbf{y} = \prod_{i=1}^{\ell} \int f(\mathbf{z}_i | \mathbf{y}_i) f(\mathbf{y}_i) d\mathbf{y} = \prod_{i=1}^{\ell} f(\mathbf{z}_i),$$

which treats the ℓ subvectors $\mathbf{z}_1, \dots, \mathbf{z}_\ell$ independently. When each block corresponds to a contiguous subregion in space, Stein (2014) showed that this approximation can be quite competitive as a surrogate for the likelihood, and also computationally inexpensive since each term in the product incurs a small computational cost and can be computed in parallel. One difficulty with this approach is characterization of joint uncertainties in predictions, due to the independence assumption embedded in the approximation.

2.4.4 Latent autoregressive process of order m (AR(m))

Latent (vector-)AR processes of order m , also called hidden Markov models or state-space models, are common in time-series settings. They condition only on the latest m sets of latent variables for some ordering: $q(i) = q_y(i) = \{i - m, \dots, i - 1\}$, or $\mathbf{x}_{p(i)} = (\mathbf{y}'_{i-m}, \dots, \mathbf{y}'_{i-1})'$. Inference in this type of model is typically carried out using the Kalman filter and smoother (Kalman, 1960; Rauch et al., 1965).

2.4.5 Modified predictive process (MPP; Finley et al., 2009)

This special case is obtained by always conditioning on the same vector \mathbf{y}_1 (with the corresponding locations \mathcal{S}_1 called “knots” in this context), and treating all other variables as conditionally independent; that is, for $i > 1$ choose $\mathbf{x}_{p(i)} = \mathbf{y}_1$ and $r_i = 1$.

2.4.6 Full-scale approximation (FSA)

The FSA-block (Snelson and Ghahramani, 2007; Sang et al., 2011) is obtained by again designating a common conditioning vector \mathbf{y}_1 , grouping all remaining variables by spatial region as in the independent-blocks case above, and choosing $\mathbf{x}_{p(i)} = \mathbf{y}_1$ for $i > 1$. In this sense, the only difference to the MPP is that for the FSA we have $r_i > 1$ in general.

To see this connection between the FSA (and its special case, the MPP) and the general Vecchia approach, note that the FSA-block approximation assumes $\widehat{\text{var}}(\mathbf{y}_i) = \text{var}(\mathbf{y}_i)$, and $\widehat{\text{cov}}(\mathbf{y}_i, \mathbf{y}_j) = \text{cov}(\mathbf{E}(\mathbf{y}_i | \mathbf{y}_1), \mathbf{E}(\mathbf{y}_j | \mathbf{y}_1))$ for $i \neq j > 1$, where $\mathbf{E}(\mathbf{y}_i | \mathbf{y}_1)$ is the predictive process with knots \mathcal{S}_1 evaluated at \mathcal{S}_i . For general Vecchia with $\mathbf{x}_{p(i)} = \mathbf{y}_1$ for all $i > 1$, we have $\widehat{f}(\mathbf{y}) = f(\mathbf{y}_1) \prod_{i=2}^{\ell} f(\mathbf{y}_i | \mathbf{y}_1)$, and so $\widehat{f}(\mathbf{y}_1) = f(\mathbf{y}_1)$, $\widehat{f}(\mathbf{y}_i) = \int f(\mathbf{y}_1) f(\mathbf{y}_i | \mathbf{y}_1) d\mathbf{y}_1 = f(\mathbf{y}_i)$ for $i > 1$ (i.e., the marginal distributions are exact), and $\widehat{f}(\mathbf{y}_i, \mathbf{y}_j) = \int f(\mathbf{y}_1) f(\mathbf{y}_i | \mathbf{y}_1) f(\mathbf{y}_j | \mathbf{y}_1) d\mathbf{y}_1$. Hence, as for the FSA, we have $\widehat{\text{var}}(\mathbf{y}_i) = \text{var}(\mathbf{y}_i)$, and for $i \neq j > 1$,

$$\begin{aligned} \widehat{\text{cov}}(\mathbf{y}_i, \mathbf{y}_j) &= \int \int \int \mathbf{y}_i \mathbf{y}_j' f(\mathbf{y}_1) f(\mathbf{y}_i | \mathbf{y}_1) f(\mathbf{y}_j | \mathbf{y}_1) d\mathbf{y}_i d\mathbf{y}_j d\mathbf{y}_1 \\ &= \int \left(\int \mathbf{y}_i f(\mathbf{y}_i | \mathbf{y}_1) d\mathbf{y}_i \right) \left(\int \mathbf{y}_j' f(\mathbf{y}_j | \mathbf{y}_1) d\mathbf{y}_j \right) f(\mathbf{y}_1) d\mathbf{y}_1 \\ &= \text{cov}(\mathbf{E}(\mathbf{y}_i | \mathbf{y}_1), \mathbf{E}(\mathbf{y}_j | \mathbf{y}_1)). \end{aligned}$$

2.4.7 Multi-resolution approximation (MRA; Katzfuss, 2017)

The MRA can be viewed as an iterative extension of the FSA-block, in which the domain \mathcal{D} is iteratively partitioned into J subregions, and we select r_i variables in each of the resulting subregions, such that $\mathcal{S}_i \subset \mathcal{D}_i$. For example, if $J = 4$, let $\mathcal{D}_1 = \mathcal{D}$, and define $\{\mathcal{D}_2, \dots, \mathcal{D}_5\}$ to be a partition of \mathcal{D}_1 , $\{\mathcal{D}_6, \dots, \mathcal{D}_9\}$ to be a partition of \mathcal{D}_2 , $\{\mathcal{D}_{10}, \dots, \mathcal{D}_{13}\}$ to be a partition of \mathcal{D}_3 , and so forth. Set $q(i) = \{j : \mathcal{D}_i \subset \mathcal{D}_j\}$, and define the conditioning vector as $\mathbf{x}_{p(i)} = \mathbf{y}_{q(i)}$, so that the conditioning vector consists of latent variables associated with locations above it in the hierarchy.

The FSA and MPP are special cases of the MRA. All three methods allow latent variables at unobserved locations, such that \mathcal{S} is different from the set of observed locations, which can be handled in our framework by a more general $\mathbf{O}_i \neq \mathbf{I}_{r_i}$.

2.4.8 Related approach: Composite likelihood

More general composite likelihood approaches (e.g., Bevilacqua et al., 2012; Eidsvik et al., 2014) also assume conditional independence and result in unbiased estimating equations, but they do not respect a particular ordering and thus can lead to improper joint distributions.

2.5 Connections to directed acyclic graphs

There are strong connections between the Vecchia approach and directed acyclic graphs (DAGs; cf. Datta et al., 2016a). We will use this connection here to illustrate different instances of the general Vecchia framework, and to study the sparsity of the matrices needed for inference in Section 3.4.

We begin with a brief review of DAGs (see, e.g., Rütimann and Bühlmann, 2009, Sect. 2). A directed graph consists of vertices, say $\{\mathbf{x}_1, \dots, \mathbf{x}_b\}$, and directed edges (i.e., arrows). Two vertices \mathbf{x}_i and \mathbf{x}_j are called adjacent if there is an edge between them. If the edge is directed from \mathbf{x}_j to \mathbf{x}_i , \mathbf{x}_j is called a parent of \mathbf{x}_i , and we write $\mathbf{x}_j \rightarrow \mathbf{x}_i$. If there is no directed edge from \mathbf{x}_j to \mathbf{x}_i , we write $\mathbf{x}_j \not\rightarrow \mathbf{x}_i$. A path Q is a sequence of adjacent vertices, and a directed path follows the direction of the arrows. A vertex \mathbf{x}_j on a path Q is said to be a collider on Q if it has converging arrows on Q (i.e., if the two edges in Q connected to \mathbf{x}_j both point toward it). If there is a directed path from \mathbf{x}_j to \mathbf{x}_i , then \mathbf{x}_i is called a descendant of \mathbf{x}_j . A directed graph is called a DAG if it does not contain directed paths for which the first and last vertices coincide.

For any three disjoint subsets $\mathcal{A}, \mathcal{B}, \mathcal{C}$ of $\{\mathbf{x}_1, \dots, \mathbf{x}_b\}$, \mathcal{A} and \mathcal{B} are called d -separated by \mathcal{C} if, for every (undirected) path Q from a vertex in \mathcal{A} to a vertex in \mathcal{B} , there is at least one vertex $\mathbf{x}_k \in \mathcal{C}$ that blocks the path in one of the following ways:

B1: \mathbf{x}_k is not a collider on Q and \mathbf{x}_k is in \mathcal{C} , or

B2: \mathbf{x}_k is a collider on Q and neither \mathbf{x}_k nor any of its descendants are in \mathcal{C} .

If \mathbf{x} follows a multivariate normal distribution (as we assume here), then \mathcal{A} and \mathcal{B} are conditionally independent given \mathcal{C} if and only if they are d -separated by \mathcal{C} .

The conditional-independence structure implied by the Vecchia approximation in (3) can be well represented by a DAG. Viewing $\{\mathbf{x}_1, \dots, \mathbf{x}_b\}$ as the vertices in the DAG, we have $\mathbf{x}_j \rightarrow \mathbf{x}_i$ if and only if $j \in g(i)$, and so $\mathbf{x}_{g(i)}$ is the vector formed by the set of all parents of

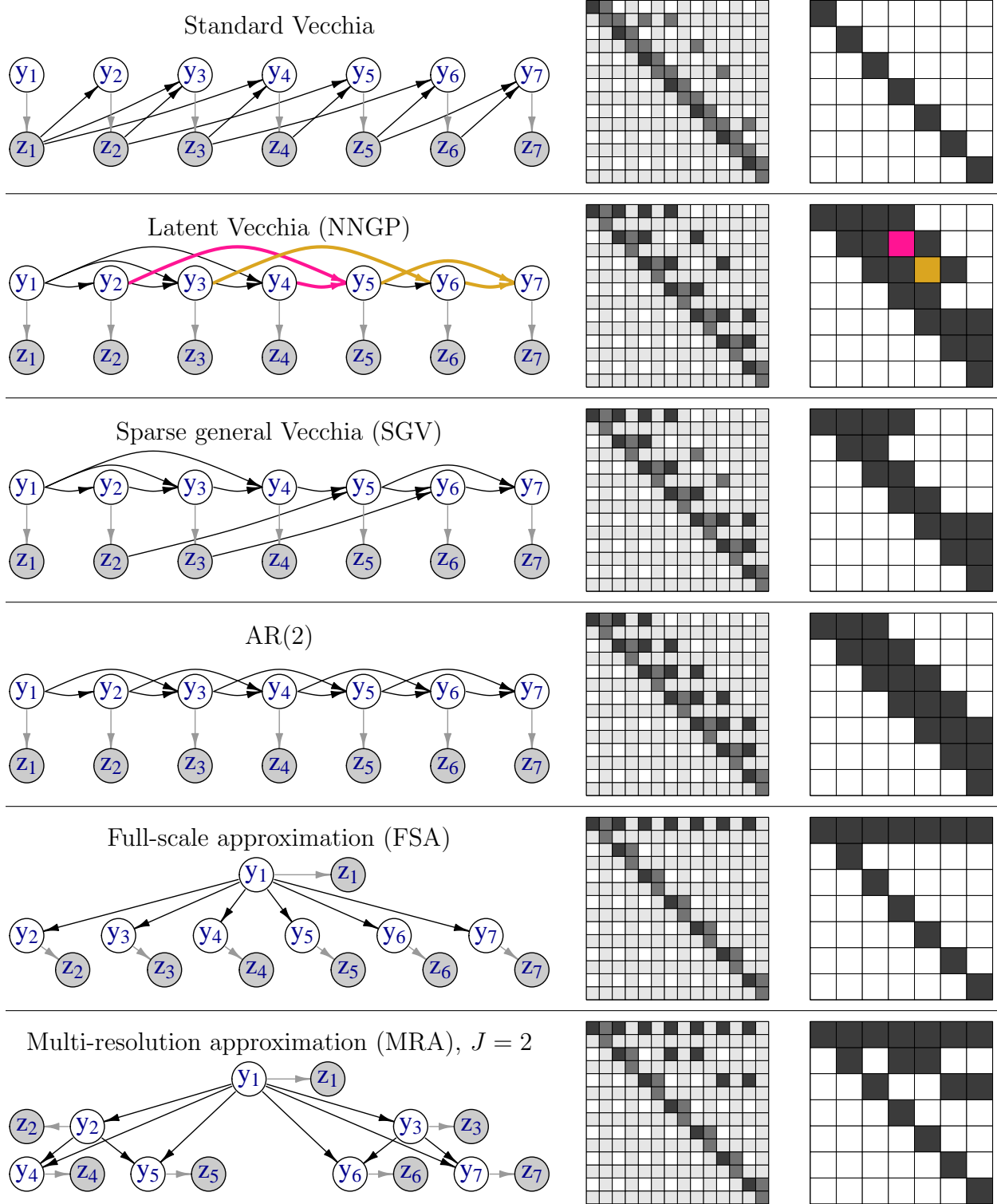


Figure 1: Toy examples of special cases of our general Vecchia approach (see Section 2.4) with $\ell = 7$, including sparse general Vecchia (Section 4). First column: DAGs (see Section 2.5). Second column: sparsity of \mathbf{U} (elements corresponding to \mathbf{z}_i in gray). Third column: sparsity of \mathbf{V} (Section 3.4). Computational complexity depends on the number of nonzero off-diagonal elements in each column of \mathbf{U} and \mathbf{V} (Section 3.5). For all methods except latent Vecchia, these numbers are at most $m = 2$. For latent Vecchia, two nonzero-producing paths and the resulting nonzero elements are highlighted (see Section 4).

\mathbf{x}_i . Note that, because Vecchia approximations allow conditioning only on previous variables in the ordering, we always have $\mathbf{x}_i \not\rightarrow \mathbf{x}_j$ if $i > j$. DAG representations are illustrated in Figure 1 for most of the approaches reviewed in Section 2.4.

3 Inference and computations

In this section, we describe matrix representations of general Vecchia approximations, which enable likelihood-based parameter inference and spatial predictions. Further, we examine the sparsity of the involved matrices and derive the computational complexity.

3.1 Matrix representations of general Vecchia

For any two subvectors \mathbf{x}_i and \mathbf{x}_j of \mathbf{x} , we write $C(\mathbf{x}_i, \mathbf{x}_j) = E(\mathbf{x}_i \mathbf{x}_j')$, the cross-covariance between \mathbf{x}_i and \mathbf{x}_j . Using the notation from Section 2.1, we have $C(\mathbf{y}_i, \mathbf{y}_j) = K(\mathcal{S}_i, \mathcal{S}_j)$, $C(\mathbf{z}_i, \mathbf{y}_j) = \mathbf{O}_j K(\mathcal{S}_i, \mathcal{S}_j)$, and $C(\mathbf{z}_i, \mathbf{z}_j) = \mathbf{O}_i K(\mathcal{S}_i, \mathcal{S}_j) \mathbf{O}_j' + \mathbb{1}_{i=j} \mathbf{R}_i$.

Then, we can write the general Vecchia approximation in (3) as

$$\hat{f}(\mathbf{x}) = \prod_{i=1}^b f(\mathbf{x}_i | \mathbf{x}_{g(i)}) = \prod_{i=1}^b \mathcal{N}(\mathbf{x}_i | \mathbf{B}_i \mathbf{x}_{g(i)}, \mathbf{D}_i) \quad (5)$$

where $\mathbf{B}_i = C(\mathbf{x}_i, \mathbf{x}_{g(i)})C(\mathbf{x}_{g(i)}, \mathbf{x}_{g(i)})^{-1}$ and $\mathbf{D}_i = C(\mathbf{x}_i, \mathbf{x}_i) - \mathbf{B}_i C(\mathbf{x}_{g(i)}, \mathbf{x}_i)$. We denote by \mathbf{B}_i^j the k th block of \mathbf{B}_i if j is the k th element in the set $g(i)$ (i.e., \mathbf{B}_i^j is the block of \mathbf{B}_i corresponding to \mathbf{x}_j).

For any symmetric, positive-definite matrix, say \mathbf{A} , let $\text{chol}(\mathbf{A})$ be the lower-triangular Cholesky factor of \mathbf{A} , and let \mathbf{P} be a permutation matrix so that $\mathbf{P}\mathbf{A}$ reorders the rows of matrix \mathbf{A} in reverse order. Then, we call $\text{rchol}(\mathbf{A}) := \mathbf{P}(\text{chol}(\mathbf{P}\mathbf{A}\mathbf{P}))\mathbf{P}$ the reverse Cholesky factor of \mathbf{A} (i.e., the row-column reverse reordering of the Cholesky factor of the row-column reverse reordering of \mathbf{A}).

PROPOSITION 1. *For the density in (5), we have $\hat{f}(\mathbf{x}) = \mathcal{N}_n(\mathbf{x} | \mathbf{0}, \hat{\mathbf{C}})$, where $\hat{\mathbf{C}}^{-1} = \mathbf{U}\mathbf{U}'$, \mathbf{U} is a sparse upper triangular block matrix with (j, i) th block*

$$\mathbf{U}_{ji} = \begin{cases} \mathbf{D}_i^{-1/2}, & i = j, \\ -(\mathbf{B}_i^j)' \mathbf{D}_i^{-1/2}, & j \in g(i), \\ \mathbf{0}, & \text{otherwise,} \end{cases} \quad (6)$$

and $\mathbf{D}_i^{-1} = \mathbf{D}_i^{-1/2}(\mathbf{D}_i^{-1/2})'$. Further, $\mathbf{U} = \text{rchol}(\hat{\mathbf{C}}^{-1})$ is the reverse Cholesky factor of $\hat{\mathbf{C}}^{-1}$.

All proofs can be found in Appendix A.

3.2 Likelihood

By integrating with respect to the latent \mathbf{y} , the general Vecchia approximation implies a distribution for the observed vector \mathbf{z} as in (4). Numerical integration is highly challenging

as \mathbf{y} is typically very high-dimensional (see Finley et al., 2017). We now provide an expression for the analytically integrated density that allows fast evaluation of the likelihood for any given value of the parameter vector $\boldsymbol{\theta}$, and thus enables likelihood-based inference for unknown parameters in the model (e.g., by numerically maximizing the likelihood, or by Metropolis-Hastings sampling from the posterior):

PROPOSITION 2. *The general Vecchia likelihood can be computed as:*

$$-2 \log \hat{f}(\mathbf{z}) = \sum_{i=1}^b \log |\mathbf{D}_i| - 2 \sum_{i=1}^{\ell} \log |\mathbf{V}_{ii}| + \tilde{\mathbf{z}}' \tilde{\mathbf{z}} - (\mathbf{V}^{-1} \mathbf{U}_y \tilde{\mathbf{z}})' (\mathbf{V}^{-1} \mathbf{U}_y \tilde{\mathbf{z}}) + n_z \log(2\pi), \quad (7)$$

where $\mathbf{V} := \text{rchol}(\mathbf{W})$, $\mathbf{W} := \mathbf{U}_y \mathbf{U}_y'$, $\tilde{\mathbf{z}} := \mathbf{U}_z' \mathbf{z}$, and \mathbf{U}_y and \mathbf{U}_z are the matrices consisting only of the rows of \mathbf{U} corresponding to \mathbf{y} and \mathbf{z} , respectively.

Note that, analogously to $\mathbf{U} = \text{rchol}(\hat{\mathbf{C}}^{-1})$ in Proposition 1, we compute $\mathbf{V} = \text{rchol}(\mathbf{W})$ as the reverse Cholesky factor of \mathbf{W} . This allows us to derive the sparsity structure of \mathbf{V} in Proposition 3 below, and ensures low computational complexity for certain configurations of general Vecchia.

3.3 Prediction

The posterior distribution of the error-free process vector is given by $\mathbf{y}|\mathbf{z} \sim \mathcal{N}(\boldsymbol{\mu}, \mathbf{W}^{-1})$, where $\boldsymbol{\mu} := -\mathbf{W}^{-1} \mathbf{U}_y \tilde{\mathbf{z}}$ (see the proof of Proposition 2). The matrix \mathbf{W} is the (sparse) joint posterior precision matrix of \mathbf{y} . If the vector \mathbf{y} contains the process of interest at all relevant spatial locations, interest is in all or parts of the posterior covariance matrix of \mathbf{y} , which is the inverse of \mathbf{W} . See Figure 2 for an illustration. Because \mathbf{W}^{-1} is generally dense, it is often infeasible to compute the entire covariance matrix, but a selected inversion algorithm (Erisman and Tinney, 1975; Li et al., 2008; Lin et al., 2011) can be used to compute $\text{cov}(\mathbf{y}_j, \mathbf{y}_i|\mathbf{z})$ for all pairs $j < i$ with $\mathbf{y}_j \rightarrow \mathbf{y}_i$. Hence, this algorithm can produce prediction variances, and the prediction covariances for adjacent vertices in the DAG. In addition, we can obtain the posterior distribution of linear combinations: $\mathbf{H}\mathbf{y}|\mathbf{z} \sim \mathcal{N}(\mathbf{H}\boldsymbol{\mu}, (\mathbf{V}^{-1}\mathbf{H}')'(\mathbf{V}^{-1}\mathbf{H}'))$. As $\mathbf{V}^{-1}\mathbf{H}'$ is also generally dense, only a moderate number of linear combinations is computationally feasible.

3.4 Sparsity structures

In the following proposition, we use the connections between Vecchia approaches and DAGs (see Section 2.5) to verify the sparsity structure of \mathbf{U} in (6) and to determine the sparsity structures of \mathbf{W} and $\mathbf{V} = \text{rchol}(\mathbf{W})$, which must be computed for evaluating the likelihood and for spatial prediction. For a block matrix \mathbf{A} , denote the (j, i) th block of \mathbf{A} by \mathbf{A}_{ji} .

PROPOSITION 3.

1. $\mathbf{U}_{ji} = \mathbf{0}$ if $i \neq j$ and $\mathbf{x}_j \not\rightarrow \mathbf{x}_i$.
2. $\mathbf{W}_{ji} = \mathbf{0}$ if $i \neq j$, $\mathbf{y}_j \not\rightarrow \mathbf{y}_i$, $\mathbf{y}_i \not\rightarrow \mathbf{y}_j$, and there is no $k > \max(i, j)$ such that both $\mathbf{y}_i \rightarrow \mathbf{y}_k$ and $\mathbf{y}_j \rightarrow \mathbf{y}_k$.
3. $\mathbf{V}_{ji} = \mathbf{0}$ if $j > i$. For $j < i$, $\mathbf{V}_{ji} = \mathbf{0}$ if there is no path between \mathbf{y}_i and \mathbf{y}_j on the subgraph $\{\mathbf{y}_i, \mathbf{y}_j\} \cup \{\mathbf{y}_k : k > i, \mathbf{y}_k \text{ has at least one observed descendant}\}$.

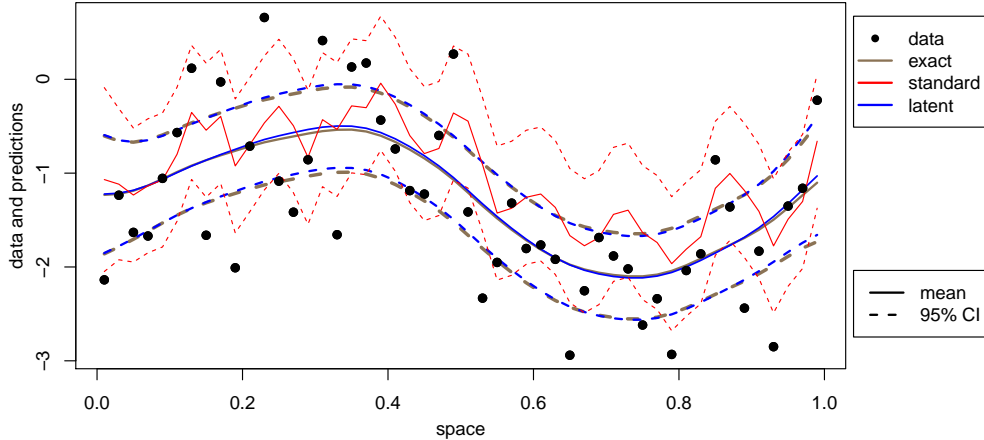


Figure 2: Posterior means and pointwise 95% credible intervals for \mathbf{y} for a GP with Matérn covariance with smoothness 1.5, effective range 0.4, and signal-to-noise ratio 1, using exact inference, and latent and standard Vecchia with $r_i = 1$, $m = 2$, left-to-right ordering, and nearest-neighbor conditioning. SGV is equivalent to latent Vecchia in this setting. Standard Vecchia assumes that y_i is conditionally dependent of all other observations given $\mathbf{z}_{(i-2):(i+2)}$, which leads to strong fluctuations of the posterior mean.

Thus, \mathbf{U} and \mathbf{V} are upper triangular, and the sparsity of the upper triangle depends on the Vecchia specification. For $j < i$, the (j, i) block of \mathbf{W} is not only nonzero if $j \in q_y(i)$, but also if \mathbf{y}_i and \mathbf{y}_j appear in a conditioning set together (i.e., $i, j \in q_y(k)$ for some k). Note that this sparsity structure corresponds to the adjacent vertices in the so-called moral graph (e.g., Lauritzen, 1996, Sect. 2.1.1). The matrix \mathbf{V} is typically at least as dense as \mathbf{W} (assuming that all or most \mathbf{y}_k have observed descendants), in that it has the same nonzeros as \mathbf{W} plus additional ones induced by more complicated paths. Figure 1 shows examples of DAGs with the corresponding sparsity structures of \mathbf{U} and \mathbf{V} .

3.5 Computational complexity

Recall that \mathbf{x} is a vector of length n , consisting of \mathbf{y} and \mathbf{z} , where $\mathbf{y} = (\mathbf{y}'_1, \dots, \mathbf{y}'_\ell)'$ and $\mathbf{z} = (\mathbf{z}'_1, \dots, \mathbf{z}'_\ell)'$, and \mathbf{y}_i and \mathbf{z}_i are of length r_i and r_i^z , respectively. To simplify the sparsity and computational complexity calculations, assume that all r_i and r_i^z are of the same order, say r (and so $n \approx br = 2\ell r$), and that all conditioning sets consist of at most m subsets (of size r): $|g(i)| \leq m$.

Then, it is easy to see from (6) that \mathbf{U} has $\mathcal{O}(b \cdot (mr^2)) = \mathcal{O}(nmr)$ nonzero elements and can be computed in $\mathcal{O}(b \cdot (m^3r^3)) = \mathcal{O}(nm^3r^2)$ time. Note that this time complexity is lower in r than in m , whose product (mr) makes up the total length of the conditioning vectors.

To evaluate the likelihood in (7) and obtain spatial predictions (see Section 3.3), we also need to compute $\mathbf{W} = \mathbf{U}_y \mathbf{U}'_y$ and find its reverse Cholesky decomposition $\mathbf{V} = \text{rchol}(\mathbf{W})$ (or the selected inverse of \mathbf{W}). Each conditioning set is of size $|g(k)| \leq m$ and so contains at most $m(m-1)/2$ pairs of elements. Therefore, from Proposition 3, \mathbf{W} has at most $\mathcal{O}(\ell m^2)$ non-zero blocks. Since each block is of size $r \times r$ and $\ell = n/r$, \mathbf{W} has at most $\mathcal{O}(nrm^2)$ non-zero elements.

The time complexity for obtaining a lower-triangular Cholesky factor is on the order of the sum of the squares of the number of nonzero elements per column in the factor (e.g.,

Toledo, 2007, Thm. 2.2). It can be easily verified that the same holds for our reordered Cholesky factorization (i.e., for \mathbf{V}). The selected inversion of \mathbf{W} for spatial prediction discussed in Section 3.3 has the same complexity as computing $\mathbf{V} = \text{rchol}(\mathbf{W})$, albeit with a higher constant (e.g., Lin et al., 2011). Thus, for any particular Vecchia approximation, the time complexity for inference can in principle be determined based on the corresponding DAG using Proposition 3, but it is difficult to give general results beyond the worst-case complexity of at least $\mathcal{O}(n^2)$ or higher (due to the possibility of $\mathcal{O}(\ell)$ nonzero blocks in at least some of the columns of \mathbf{V}). Further specific examples are given in the next section.

4 Sparse general Vecchia (SGV) approximation

We now study choice C5 from Section 2.3 for fixed choices C1–C4; that is, we assume that the grouping, ordering, and the conditioning index sets $q(1), \dots, q(\ell)$ are fixed. We consider three methods that differ in their choice of latent versus observed conditioning (C5): the existing methods standard Vecchia (Section 2.4.1) and latent Vecchia (used in the NNGP in Section 2.4.2), and a novel sparse general Vecchia (SGV) approach:

Standard Vecchia (\hat{f}_s): $q_z(i) = q(i)$, and so $\mathbf{x}_{p(i)} = \mathbf{z}_{q(i)}$.

Latent Vecchia (\hat{f}_l): $q_y(i) = q(i)$, and so $\mathbf{x}_{p(i)} = \mathbf{y}_{q(i)}$.

SGV (\hat{f}_g): For each i , partition $q(i)$ into $q_y(i)$ and $q_z(i)$ such that j and k with $j < k$ can only both be in $q_y(i)$ if $j \in q_y(k)$.

In the terminology of Lauritzen (1996, Sect. 2.1.1), SGV ensures that the corresponding DAG forms a perfect graph. Different versions of SGV are possible for the same conditioning index sets (and, in fact, standard Vecchia is one special case of SGV). Throughout this article, in the SGV we obtain $q_y(i)$ for each $i = 2, \dots, \ell$ as $q_y(i) = \{k\} \cup (q_y(k) \cap q(i))$, where k is chosen as the index in the set $\arg \max_{j \in q(i)} |q_y(j) \cap q(i)|$ for which the spatial distance between \mathcal{S}_i and \mathcal{S}_k is shortest.

The three approaches are illustrated in a toy example with $l = 7$ shown in Figure 1. For all three methods we have the same $q(1), \dots, q(\ell)$: $q(2) = \{1\}$, $q(3) = \{1, 2\}$, $q(4) = \{1, 3\}$, $q(5) = \{2, 4\}$, \dots . Like latent Vecchia, SGV uses $q_y(2) = \{1\}$, $q_y(3) = \{1, 2\}$, $q_y(4) = \{1, 3\}$, as, for example, $1 \in q_y(3)$, and so $q_y(4)$ can contain both 1 and 3. However, $2 \notin q_y(4)$, and so SGV does not allow both $2 \in q_y(5)$ and $4 \in q_y(5)$, and sets $q_y(5) = \{4\}$ and $q_z(5) = \{2\}$.

PROPOSITION 4. *The following ordering of Kullback-Leibler (KL) divergences holds:*

$$\text{KL}(f(\mathbf{x}) \| \hat{f}_l(\mathbf{x})) \leq \text{KL}(f(\mathbf{x}) \| \hat{f}_g(\mathbf{x})) \leq \text{KL}(f(\mathbf{x}) \| \hat{f}_s(\mathbf{x})).$$

Thus, the approximation accuracy for the joint distribution of \mathbf{x} is better for latent Vecchia than for SGV, which is better than that for standard Vecchia. Note, however, that this does not guarantee that the KL divergence for the implied distribution of the observations \mathbf{z} follows the same ordering. See Section 6 for numerical examples.

Another important factor is the computational complexity of the different approaches. Standard Vecchia only conditions on observed quantities, and so for any i, j we have $\mathbf{y}_j \not\rightarrow \mathbf{y}_i$,

resulting in a diagonal \mathbf{W} and \mathbf{V} according to Proposition 3, and hence an overall time complexity of $\mathcal{O}(nm^3r^2)$ for standard Vecchia.

Finley et al. (2017) observed numerically that matrices in the NNGP (which uses the latent Vecchia approach) were less sparse than in standard Vecchia. We can examine this issue further using Proposition 3. In the toy example in Figure 1, latent Vecchia uses $q_y(5) = \{2, 4\}$, which creates the unblocked path $(\mathbf{y}_2, \mathbf{y}_5, \mathbf{y}_4)$ that leads to $\mathbf{V}_{2,4} \neq \mathbf{0}$. Setting $q_y(6) = \{3, 5\}$ creates the unblocked path $(\mathbf{y}_3, \mathbf{y}_6, \mathbf{y}_7, \mathbf{y}_5)$, leading to $\mathbf{V}_{3,5} \neq \mathbf{0}$. This results in $3 > m = 2$ nonzero off-diagonal elements in columns 4 and 5. We provide more insight into the increased computational cost for latent Vecchia in the following proposition:

PROPOSITION 5. *Consider the latent Vecchia approach with $r_i = r_i^z = 1$, $m = o(n^{1/d})$, and coordinate-wise ordering for locations on an equidistant grid in a d -dimensional hypercube with nearest-neighbor conditioning. Then, $\mathbf{V} = \text{rchol}(\mathbf{W})$ has $\mathcal{O}(n^{1-1/d}m^{1/d})$ nonzero elements per column, requiring $\mathcal{O}(n^{2-1/d}m^{1/d})$ memory. The resulting time complexity for computing \mathbf{V} from \mathbf{W} is $\mathcal{O}(n^{3-2/d}m^{2/d})$.*

Thus, the time complexity for obtaining \mathbf{V} is $\mathcal{O}(nm^2)$ in $d = 1$ dimensions, $\mathcal{O}(n^2m)$ for $d = 2$, and approaching the cubic complexity in n of the original GP as d increases. For irregular observation locations, we expect roughly similar scaling if the locations can be considered to have been drawn from independent uniform distributions over the domain. Also note that using reordering algorithms for the Cholesky decomposition (as opposed to simple reverse ordering) could lead to different complexities, although our numerical results indicate that this might actually increase the computational complexity (see Figure 6b).

In contrast to latent Vecchia, SGV results in guaranteed sparsity. In the toy example, SGV sets $q_y(5) = \{4\}$ and $q_z(5) = \{2\}$ because $2 \notin q_y(4)$, and $q_y(6) = \{5\}$ and $q_z(6) = \{3\}$ because $3 \notin q_y(5)$, resulting in $\mathbf{V}_{2,4} = \mathbf{V}_{3,5} = \mathbf{0}$ (in contrast to latent Vecchia). More generally, SGV preserves the linear scaling of standard Vecchia:

PROPOSITION 6. *For SGV, \mathbf{V} has at most mr off-diagonal elements per column, and so the time complexity for computing $\mathbf{V} = \text{rchol}(\mathbf{W})$ is only $\mathcal{O}(nm^2r^2)$. Thus, SGV has the same computational complexity as standard Vecchia.*

In summary, SGV provides improvements in approximation accuracy over standard Vecchia (Proposition 4) while retaining linear computational complexity in n (Proposition 6). Latent Vecchia results in improved approximation accuracy but can raise the computational complexity severely (Proposition 5), which can be infeasible for large n . Numerical illustrations of these results can be found in Section 6.

5 Ordering and conditioning

We now provide some insight into choices C2–C4 of Section 2.3. For simplicity, we henceforth assume $r_i \equiv 1$ unless stated otherwise.

5.1 Ordering (C3)

In one spatial dimension, a “left-to-right” ordering of the locations in \mathcal{S} is natural. However, in two or more spatial dimensions, it is not obvious how the locations should be ordered.

For Vecchia approaches, the default and most popular ordering is along one of the spatial coordinates (coord ordering). Datta et al. (2016a) have stated that the ordering of the locations has a negligible effect on the quality of the Vecchia approximation, but Guinness (2016) showed that this is not always true. He proposed different ordering schemes, including an approximate maximum-minimum-distance (maxmin) ordering, which sequentially picks each location in the ordering by aiming to maximize the distance to the nearest of the previous locations. Guinness (2016) showed that maxmin ordering can lead to substantial improvements over coord ordering in settings without any nugget or noise. We will examine the nonzero nugget case in Section 6. Note that the MRA (Section 2.4.7) implies an ordering scheme similar to maxmin, starting with a coarse grid over space and subsequently getting denser and denser.

5.2 Choosing m

For a given ordering, as part of C4 we must choose m , the size of the conditioning sets.

For one-dimensional spatial domains, some guidance can be obtained by considering approximating a GP with a Matérn covariance on a one-dimensional domain. If the smoothness is $\nu = 0.5$, we have a Markov process of order 1, and so we can get an exact approximation for latent conditioning with $m = 1$ by ordering from left to right. Stein (2011) conjectures that for smoothness ν , approximate screening holds for any $m > \nu$. This conjecture is explored numerically in Section 6, specifically in Figure 3a. Note that coord ordering in 1-D with m -nearest-neighbor conditioning amounts to an AR(m) model, and the corresponding latent or SGV inference is equivalent to a Kalman filter and smoother (cf. Eubank and Wang, 2002). See Figure 2 for an illustration. For very smooth processes (i.e., very large ν), the m necessary for (approximate) screening won't be affordable any more, and alternative ordering and conditioning strategies might be required (see Section 5.3 below).

For two or more dimensions, the necessary m will depend not only on the smoothness of the covariance function, but also on the chosen ordering, the observation locations (regular or irregular), and other factors. We suggest starting with a relatively small m and gradually increasing it, until the desired inference has “converged,” or until the available computational resources have been exhausted.

5.3 Same conditioning sets

For a given ordering and m , the most common strategy is to simply condition on the m nearest neighbors or locations (NN conditioning), although more elaborate conditioning schemes have been proposed (e.g., Stein et al., 2004; Gramacy and Apley, 2015). It can also be advantageous in some situations to place a coarse grid over space at the beginning of the ordering and to always condition on this set, so that all conditioning vectors consist solely of \mathbf{y}_1 , of size r_1 ; that is, $p(i) = \{1\}$ for all $i > 1$. This is the strategy employed by the MPP and FSA in Sections 2.4.5–2.4.6 with $r_i = 1$ and $r_i = r$, respectively, for $i > 1$. For example, one could choose the first r_1 variables in the maxmin ordering, which result in a coarse grid over \mathcal{D} .

This same-conditioning-set (SCS) approach has several advantages. First, SGV is equivalent to latent Vecchia for SCS; or, in other words, the sparsity for the latent approach can

be guaranteed. Second, as discussed in Section 5.2 above, if smoothness and range are large enough, no screening effect will hold. SCS is an extension of the predictive process, which tends to work well in such “smooth” situations, because it is equivalent to a Nyström approximation of the leading terms of the Karhunen-Loève expansion of $y(\cdot)$ (Sang and Huang, 2012). Third, a lower computational complexity can be achieved, because $C(\mathbf{x}_{p(i)}, \mathbf{x}_{p(i)}) = C(\mathbf{y}_1, \mathbf{y}_1)$ in (5) is the same matrix for all $i = 2, \dots, l$ and its Cholesky decomposition only needs to be computed once. Assuming $r_1 = rm$, the cost of the Cholesky decomposition is $\mathcal{O}((rm)^3)$, and each \mathbf{B}_i and \mathbf{D}_i can be computed in $\mathcal{O}(r_i^3 m^2)$ time, resulting in an overall time complexity for SCS of $\mathcal{O}(nm^2 r^2)$ (i.e., reduced by factor m relative to the general case) for $r_i = r$ for $i > 1$. Fourth, the marginal distributions the \mathbf{x}_i (and hence also the variances) are exact (see Section 2.4.6). Fifth, it is straightforward to show that \mathbf{V}^{-1} has the same sparsity structure as \mathbf{V} , which allows fast calculation of the joint posterior predictive distribution for a large number of prediction locations, and extension to Kalman-filter-type inference for massive spatio-temporal data (Jurek and Katzfuss, in preparation). Note that all of these advantages also hold for the MRA, which can be viewed as an iterative SCS approach at multiple resolutions (Katzfuss, 2017, Jurek and Katzfuss, in preparation).

6 Numerical study

We now illustrate numerically the propositions and claims made in previous sections. We explored C3–C5 from Section 2.3, and compared the three approaches from Section 4. Throughout this section, we set $r_i = 1$ and $\mathbf{O}_i = 1$, the observation locations were given by equidistant grids on the unit interval or unit square, and the true GP was assumed to have Matérn covariance with variance σ^2 , smoothness ν , and effective range λ (i.e., the distance at which the correlation drops to 0.05). We added noise with variance $\mathbf{R}_i = \tau^2$, set $\sigma^2 + \tau^2 = 1$, and so the signal proportion was $\sigma^2/(\sigma^2 + \tau^2) = \sigma^2$. For example, signal proportions of 1/2 and 2/3 correspond to signal-to-noise ratios (SNRs) of 1 and 2, respectively. We considered coordinate-wise (coord) ordering and the approximate maximum-minimum-distance (maxmin) ordering of Guinness (2016). We used nearest-neighbor (NN) conditioning for a given ordering, unless stated otherwise. Comparisons among methods are made using the Kullback-Leibler (KL) divergence between the approximate distribution $\hat{f}(\mathbf{z})$ and the true distribution $f(\mathbf{z})$.

First, we assumed a one-dimensional spatial domain, $\mathcal{D} = [0, 1]$, and only considered the natural coord ordering “from left to right.” The different methods from Section 4 then essentially correspond to (latent or non-latent) AR(m) processes. From the results shown in Figure 3 with $n_z = 100$ and $\lambda = 0.9$, we can see that latent Vecchia (and hence the equivalent SGV) performed much better than standard Vecchia. Figure 3a also confirms numerically the conjecture from Section 5 that (approximate) screening holds if $m > \nu$ (for latent Vecchia). Predictions in this setting were shown in Figure 2.

The remaining results are for a two-dimensional domain, $\mathcal{D} = [0, 1]^2$. Exploring Proposition 4, Figure 4 shows KL divergences for different values of σ^2 , ν , and m , all for $n_z = 6,400$ and $\lambda = 0.9$. As we can see, the KL divergences for the three methods roughly followed the ordering from Section 4, with latent Vecchia performing better than SGV, which performed better than standard Vecchia. (For SNR= ∞ , the methods are equivalent.) The

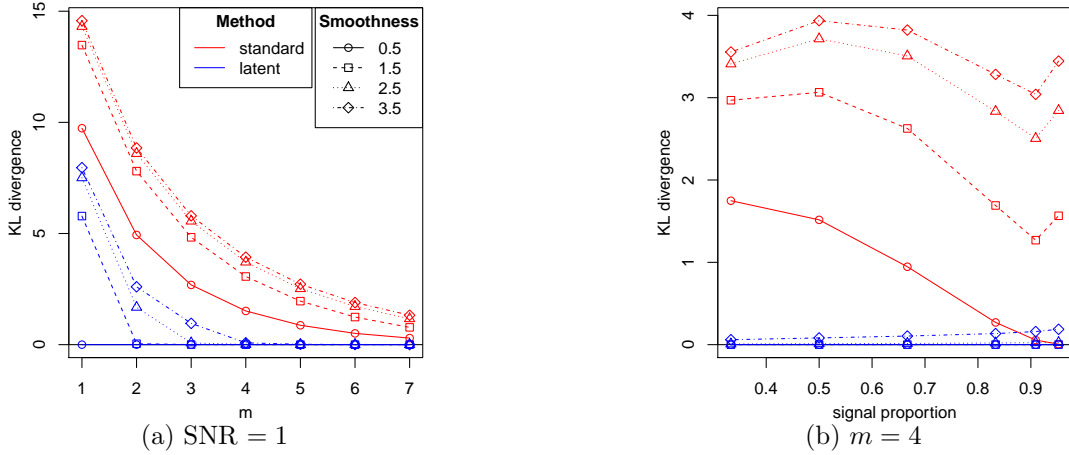


Figure 3: KL divergences for Vecchia approximations of a GP with Matérn covariance on the unit interval with coord ordering and NN conditioning. SGV is equivalent to latent Vecchia in this setting.

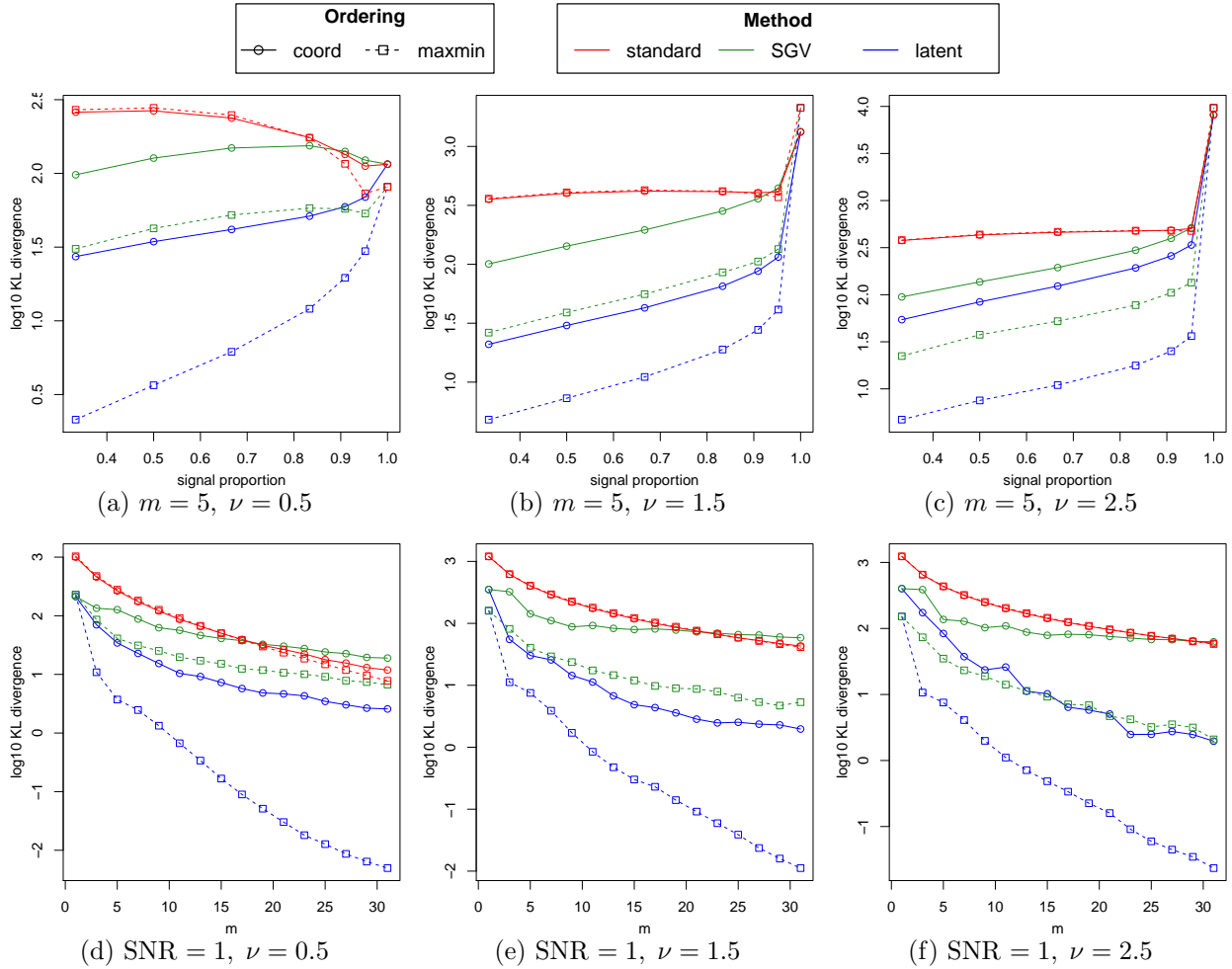


Figure 4: KL divergences (on a log scale) for a Matérn covariance with smoothness ν on the unit square. Panels (a)–(c): fixed $m = 5$, varying signal proportion, with symbols corresponding to (from left to right) SNRs of 0.5, 1, 2, 5, 10, 20, ∞ , respectively. Panels (d)–(f): fixed SNR = 1, varying m .

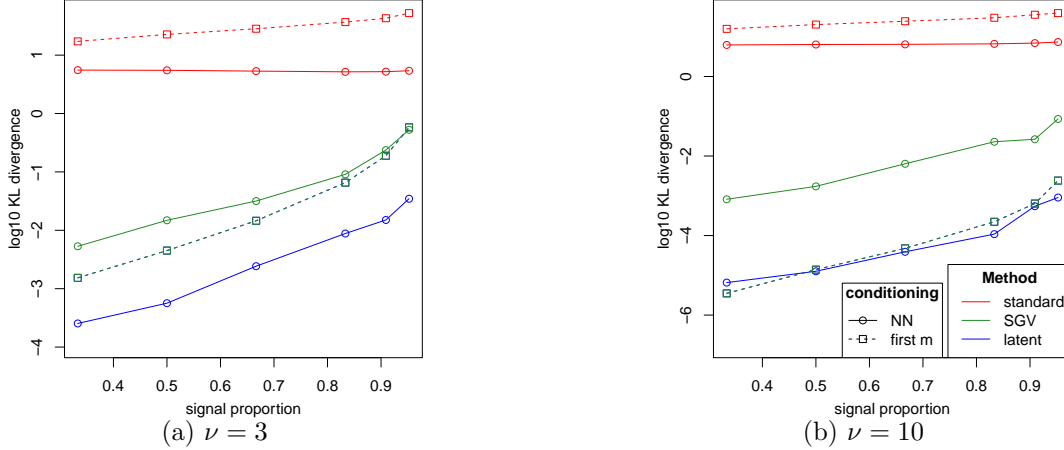


Figure 5: KL divergences (on a log scale) for smooth covariances, comparing nearest-neighbor (NN) conditioning versus always choosing the first- m variables; $n_z = 400$, $m = 16$, maxmin ordering, $\lambda \approx 2$. For first- m conditioning, SGV and latent are equivalent.

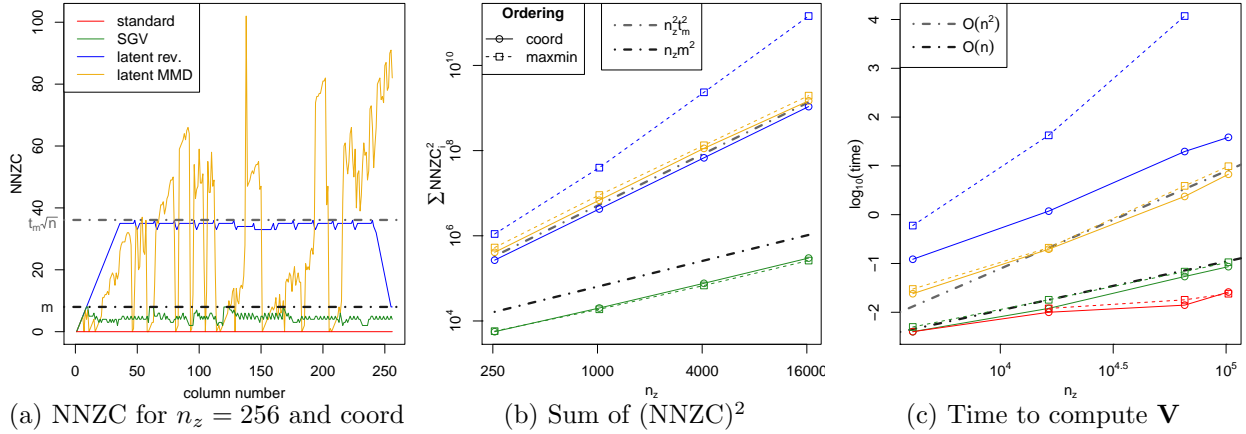


Figure 6: Sparsity, complexity, and actual computation times of obtaining \mathbf{V} with $m = 8$, and so $t_m = (2m/\pi)^{1/2} \approx 2.25$ (see proof of Proposition 5). NNZC: number of nonzero off-diagonal elements per column in \mathbf{V} ; MMD and rev.: multiple minimum degree and reverse ordering, respectively, for Cholesky algorithm

screening effect (seen in 1-D in Figure 3a) is less clear in two dimensions. Also note that maxmin ordering often resulted in tremendous improvements over coord ordering, except for standard Vecchia, where the two orderings produced similar results.

We also considered very smooth covariances, which are less common in geostatistics but very popular in machine learning. We explored conditioning on the same set, chosen as the first m variables in the maxmin ordering, which spreads the observations throughout the domain. Figure 5 shows that this can result in strong improvements over NN ordering for SGV.

The computational feasibility of the methods is explored in Figure 6, which examines the sparsity of the matrix \mathbf{V} . We can see that SGV keeps the number of nonzero elements per column in \mathbf{V} at or below m , as would be expected from Proposition 6, resulting in linear scaling as a function of n . For latent Vecchia, \mathbf{V} is considerably denser, and the computational complexity for obtaining \mathbf{V} scales roughly as $O(n^2)$, as expected from Proposition

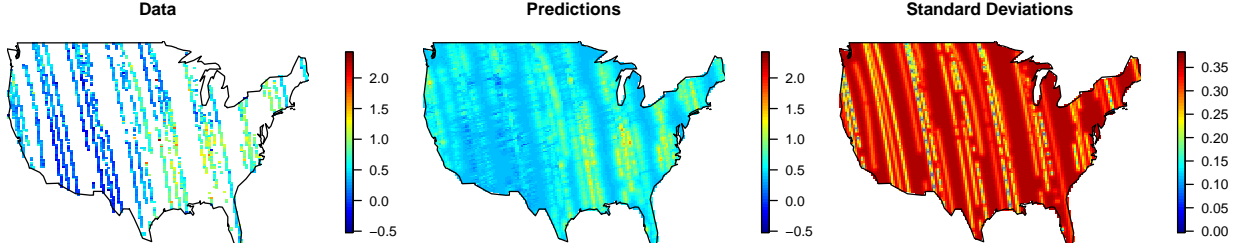


Figure 7: Satellite data, together with predictions using fitted SGV model with $m = 15$

5. MMD ordering did not improve the complexity. Figure 6c shows actual computation times for obtaining \mathbf{V} from \mathbf{W} using the `chol` function in the R package `spam` (Furrer and Sain, 2010) on a 4-core machine (Intel Core i7-3770) with 3.4GHz and 16GB RAM. Despite the `chol` function being more highly optimized for the (default) MMD ordering than the (user-supplied) reverse ordering, latent Vecchia with MMD ordering is roughly two orders of magnitude slower than SGV with reverse ordering for n_z around 100,000.

7 Application to satellite measurements of chlorophyll fluorescence

We applied some of the discussed methods to Level-2 bias-corrected solar-induced chlorophyll fluorescence retrievals over land from the Orbiting Carbon Observatory 2 (OCO-2) satellite (OCO-2 Science Team et al., 2015). The OCO-2 satellite has a sun-synchronous orbit with a period of 99 minutes and repeats its spatial coverage every 16 days. We analyzed chlorophyll fluorescence data collected during one repeat cycle from May 16 to May 31, 2017 over the contiguous United States. During this time period, there are a total of 104,683 observations, plotted in the left panel of Figure 7. There was little evidence of temporal change during the time period, so we restricted our attention to a purely spatial model.

We assumed that the (mean-corrected) data \mathbf{z} were noisy observations of the true chlorophyll fluorescence field $y(\cdot) \sim GP(0, K)$, where K is an isotropic Matérn covariance function. To speed the computations, we only considered smoothness parameters $\nu = 1/2$ and $\nu = 3/2$ resulting in a nondifferentiable and a once-differentiable model, respectively, because the Matérn has a closed form in those cases. As the choice $\nu = 1/2$ provided better fits in all settings, we ended up with the covariance function $K(\mathbf{s}_1, \mathbf{s}_2) = \sigma^2 \exp(\|\mathbf{s}_1 - \mathbf{s}_2\|/\alpha)$, $\mathbf{s}_1, \mathbf{s}_2 \in \mathcal{D}$.

We considered the two scalable versions of general Vecchia from Section 4, standard Vecchia and SGV, with $r_i = 1$, $\mathbf{O}_i = \mathbf{1}$, and $\mathbf{R}_i = \tau^2$. We used a maxmin ordering in time, as suggested by Guinness (2016) for polar-orbiting satellite data, and the conditioning sets $q(i)$ were formed using the nearest m previously ordered locations.

Figure 8 shows the loglikelihoods achieved after optimization over σ^2 , α , and τ^2 for different conditioning-set sizes m . For standard Vecchia, the fits improve as m increases; this is expected since increasing the number of neighbors leads to sharper ordered predictions and higher loglikelihoods. SGV achieved considerably higher likelihoods for small m , with no substantial improvement after $m = 10$, which suggests that conditioning on some latent variables serves to concentrate the dependence of each observation on just a small number

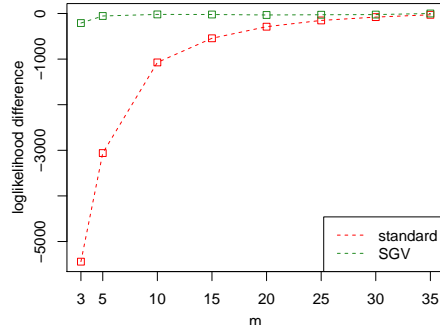


Figure 8: Loglikelihoods of fitted models (differences from best-fitting model) for satellite data

of previous latent and observed variables. Note that the difference between achieving a high likelihood with $m = 10$ (SGV) and $m = 35$ (standard) is very significant due to the cubic scaling in m .

Figure 7 shows predicted values (i.e., posterior means of $y(\mathcal{S}^P)$) and posterior standard deviations on a grid \mathcal{S}^P of 13,795 locations within the contiguous United States, under the fitted SGV model with $m = 15$. The estimated parameters for this model are $\hat{\sigma}^2 = 0.103$, $\hat{\alpha} = 47.7$ km, and $\hat{\tau}^2 = 0.162$. The standard deviations reflect the nature of the data locations; there are streaks of high standard deviations where no data were collected during the observation period.

8 Conclusions and guidelines

We have presented a general class of sparse GP approximations based on applying Vecchia’s approximation to a vector consisting of GP evaluations and their corresponding noisy observations. Several of the most commonly used GP approximations proposed in the literature are special cases of our class. We provided computationally efficient formulas for computing likelihoods and predictions, and we studied the sparsity and computational complexity using connections between (general) Vecchia approaches and directed acyclic graphs. We proposed a novel sparse general Vecchia (SGV), which can dramatically improve upon the approximation accuracy of standard Vecchia while maintaining its linear computational complexity. In contrast, we showed that latent Vecchia (which is used in the nearest-neighbor GP) can scale quadratically in the data size in two-dimensional space.

We now give some guidelines for using the general Vecchia approach in different situations. In general, we recommend using our SGV approach in the presence of nugget or noise, and the standard Vecchia directly on the observations if the noise term is zero or almost zero. In one spatial dimension, left-to-right ordering and nearest-neighbor conditioning is most natural, and SGV is equivalent to latent. In addition, the size m of the conditioning set can be chosen according to the smoothness (i.e., differentiability at the origin) of the covariance function. In two-dimensional space, we recommend maxmin ordering. While it is difficult to determine a suitable m a priori, a useful approach is to carry out inference for small m , and then gradually increase m until the inference converges or the computational resources are exhausted. Nearest-neighbor conditioning is suitable for low smoothness, while always conditioning on the first m latent variables is preferable for higher smoothness when there is

a large nugget. This first- m conditioning and its extensions (such as the MRA) has benefits beyond approximation accuracy, such as reduced computational complexity, exact marginal distributions for all variables, and sparse Cholesky factor of the posterior covariance matrix.

There are several other issues that have been mentioned here, but whose thorough investigation is beyond the scope of this article. These include the size of the partitions or groups, the inclusion of latent variables at unobserved locations (as suggested in, e.g., Datta et al., 2016a), parallel and distributed computation, and details of how the different methods differ in their ability to produce accurate (joint) predictions.

Acknowledgments

Katzfuss' research was partially supported by National Science Foundation (NSF) Grant DMS-1521676 and NSF CAREER Grant DMS-1654083. Guinness' research was partially supported by NSF Grant DMS-1613219. The authors also acknowledge support from the NSF Research Network for Statistical Methods for Atmospheric and Oceanic Sciences, No. 1107046.

A Proofs

In this section, we provide proofs for the propositions stated throughout the article.

Proof of Proposition 1. For the density in (5), we have $\hat{f}(\mathbf{x}) \propto \exp(-w/2)$, where $w = \sum_{i=1}^b \mathbf{a}'_i \mathbf{a}_i$ and

$$\mathbf{a}_i = (\mathbf{D}_i^{-1/2})'(\mathbf{x}_i - \mathbf{B}_i \mathbf{x}_{g(i)}) = (\mathbf{D}_i^{-1/2})' \mathbf{x}_i + \sum_{j \in g(i)} (-\mathbf{D}_i^{-1/2})' \mathbf{B}_i^j \mathbf{x}_j = \sum_{j=1}^b \mathbf{U}'_{ji} \mathbf{x}_j,$$

with \mathbf{U} defined as in (6). Hence, $w = \sum_{i=1}^b (\mathbf{U}'_i \mathbf{x})' (\mathbf{U}_i \mathbf{x}) = \mathbf{x}' \mathbf{U} \mathbf{U}' \mathbf{x}$, where \mathbf{U}_i is the i th block of columns in \mathbf{U} . Because \mathbf{U} is a nonsingular matrix, we have $\hat{f}(\mathbf{x}) = \mathcal{N}_n(\mathbf{x} | \mathbf{0}, \hat{\mathbf{C}})$ with $\hat{\mathbf{C}}^{-1} = \mathbf{U} \mathbf{U}'$, which proves the first part of the proposition. Note that a proof for a similar expression of the approximate joint density can be found in Datta et al. (2016a, App. A2).

Then, because \mathbf{P} is a symmetric matrix, we have $\mathbf{P} = \mathbf{P}' = \mathbf{P}^{-1}$ (and \mathbf{PMP} results in reverse row-column ordering of the square matrix \mathbf{M}). Thus, we can write $\mathbf{P} \hat{\mathbf{C}}^{-1} \mathbf{P} = \mathbf{P} \mathbf{U} \mathbf{U}' \mathbf{P} = \mathbf{P} \mathbf{U} \mathbf{P} \mathbf{P}' \mathbf{U}' \mathbf{P} = (\mathbf{P} \mathbf{U} \mathbf{P}) (\mathbf{P} \mathbf{U}' \mathbf{P})'$. The matrix $\mathbf{P} \mathbf{U} \mathbf{P}$ is lower triangular with positive values on the diagonal, and so it must be the Cholesky factor of $\mathbf{P} \hat{\mathbf{C}}^{-1} \mathbf{P}$ since the Cholesky factor is the unique such lower triangular matrix. Therefore, we have $\mathbf{U} = \mathbf{P} \text{chol}(\mathbf{P} \hat{\mathbf{C}}^{-1} \mathbf{P}) \mathbf{P} = \text{rchol}(\hat{\mathbf{C}}^{-1})$. \square

Proof of Proposition 2. By rearranging the definition of a conditional density, we obtain $\hat{f}(\mathbf{z}) = \hat{f}(\mathbf{x}) / \hat{f}(\mathbf{y} | \mathbf{z})$, which holds for any \mathbf{y} , and so we simply set $\mathbf{y} = \mathbf{0}$. Letting \mathbf{x}_0 be \mathbf{x} with $\mathbf{y} = \mathbf{0}$, we have

$$\hat{f}(\mathbf{z}) = \frac{\mathcal{N}(\mathbf{x}_0 | \mathbf{0}, \hat{\mathbf{C}})}{\mathcal{N}(\mathbf{0} | \boldsymbol{\mu}, \mathbf{W}^{-1})}, \quad (8)$$

where $\boldsymbol{\mu} := \mathbf{E}(\mathbf{y} | \mathbf{z})$ and $\mathbf{W} := \text{var}(\mathbf{y} | \mathbf{z})^{-1}$. For the numerator in (8), using the factorization $\hat{\mathbf{C}}^{-1} = \mathbf{U} \mathbf{U}'$ supplied by the Vecchia approach, we have $\log |\hat{\mathbf{C}}| = -2 \log |\mathbf{U}| = \sum_{i=1}^b \log |\mathbf{D}_i|$ and $\mathbf{x}'_0 \hat{\mathbf{C}}^{-1} \mathbf{x}_0 = (\mathbf{U}' \mathbf{x}_0)' (\mathbf{U}' \mathbf{x}_0) = \tilde{\mathbf{z}}' \tilde{\mathbf{z}}$.

For the denominator in (8), according to Theorem 12.2 in Rue and Held (2010), we have $\mathbf{W} = \mathbf{U}_y \mathbf{U}'_y$ and $\boldsymbol{\mu} = -\mathbf{W}^{-1} \mathbf{U}_y \mathbf{U}'_z \mathbf{z}$. Because $\mathbf{W} = \mathbf{V} \mathbf{V}'$ and \mathbf{V} is upper triangular, we have $\log |\mathbf{W}^{-1}| = -2 \log |\mathbf{V}| = -2 \sum_i \log |\mathbf{V}_{ii}|$. The quadratic form can be obtained as $\boldsymbol{\mu}' \mathbf{W} \boldsymbol{\mu} = \tilde{\mathbf{z}}' \mathbf{U}'_y \mathbf{W}^{-1} \mathbf{W} \mathbf{W}^{-1} \mathbf{U}_y \tilde{\mathbf{z}} = (\mathbf{V}^{-1} \mathbf{U}_y \tilde{\mathbf{z}})' (\mathbf{V}^{-1} \mathbf{U}_y \tilde{\mathbf{z}})$. \square

Proof of Proposition 3. It can be easily verified that $\text{rchol}(\mathbf{A}) = \mathbf{P}(\text{chol}(\mathbf{PAP}))\mathbf{P}$ is a lower-triangular matrix for any symmetric, positive-definite \mathbf{A} , because $\text{chol}(\cdot)$ was defined to return the lower-triangular Cholesky

factor. Hence, both $\mathbf{U} = \text{rchol}(\mathbf{C}^{-1})$ and $\mathbf{V} = \text{rchol}(\mathbf{W})$ are lower triangular. Further, $\mathbf{W} = \mathbf{U}_y \mathbf{U}'_y$ is symmetric. Therefore, we only consider the case $j < i$ in the remainder of this proof.

It is well known for precision matrices in multivariate normal distributions (e.g., Rue and Held, 2010, Thm. 12.1) that $\mathbf{W}_{ji} = \mathbf{0}$ if \mathbf{y}_i and \mathbf{y}_j are conditionally independent given all other variables in the model (i.e., conditional on $\mathcal{C}_W = \{\mathbf{y}_{-ij}, \mathbf{z}\}$). A similar result for the sparsity of the Cholesky factor (e.g., Rue and Held, 2010, Thm. 12.5) can be rephrased for our reverse Cholesky decomposition ($\mathbf{U} = \text{rchol}(\widehat{\mathbf{C}}^{-1})$) to say that $\mathbf{U}_{ji} = \mathbf{0}$ if \mathbf{x}_j and \mathbf{x}_i are conditionally independent given $\mathcal{C}_U = \{\mathbf{x}_{h(i)\setminus\{j\}}\}$. For \mathbf{V} , which is the Cholesky factor of the posterior precision matrix \mathbf{W} (i.e., conditional on \mathbf{z}), we have $\mathbf{V}_{ji} = \mathbf{0}$ if \mathbf{y}_i and \mathbf{y}_j are conditionally independent given $\mathcal{C}_V = \{\mathbf{y}_{h(i)\setminus\{j\}}, \mathbf{z}\}$. Thus, $\mathbf{U}_{ji} = \mathbf{0}$ if and only if \mathbf{x}_i and \mathbf{x}_j are d -separated by \mathcal{C}_U in the DAG, and $\mathbf{W}_{ji} = \mathbf{0}$ and $\mathbf{V}_{ji} = \mathbf{0}$ if and only if \mathbf{y}_i and \mathbf{y}_j are d -separated by \mathcal{C}_W and \mathcal{C}_V , respectively.

Note that d -separation cannot hold if $\mathbf{x}_j \rightarrow \mathbf{x}_i$, and so we only consider (paths between) non-adjacent \mathbf{x}_j and \mathbf{x}_i in the remainder of the proof. Any path between such \mathbf{x}_j and \mathbf{x}_i must pass through at least one non-collider \mathbf{x}_l with $l < i$, or through a collider \mathbf{y}_k with $2k - 1 > i$, because arrows in the Vecchia approach can only go forward in the ordering and the only parent for each \mathbf{z}_k is \mathbf{y}_k . As we have $\mathcal{C}_U = \{\mathbf{x}_l : l < i, l \neq j\}$, this means that any path between (non-adjacent) \mathbf{x}_i and \mathbf{x}_j is either blocked by a non-collider $\mathbf{x}_l \in \mathcal{C}_U$ (condition B1) or by a collider $\mathbf{x}_k \notin \mathcal{C}_U$ (B2), which proves part 1. of the proposition.

For \mathbf{W} , as all vertices other than \mathbf{y}_i and \mathbf{y}_j are in \mathcal{C}_W , we only need to consider condition B1. The only paths between \mathbf{y}_j and \mathbf{y}_i that do not contain a vertex $\mathbf{x}_k \in \mathcal{C}_W$ that is not a collider (and hence blocks the path), are paths of the form $(\mathbf{y}_j, \mathbf{y}_k, \mathbf{y}_i)$ with $\mathbf{y}_j \rightarrow \mathbf{y}_k$ and $\mathbf{y}_i \rightarrow \mathbf{y}_k$. This proves part 2.

For \mathbf{V} , any path between \mathbf{y}_i and \mathbf{y}_j that passes through $\mathcal{C}_V = \{\mathbf{y}_{h(i)\setminus\{j\}}, \mathbf{z}\}$ includes a non-collider in \mathcal{C}_V and is thus blocked (B1). Thus, \mathbf{V}_{ji} can only be nonzero if there is a path between \mathbf{y}_i and \mathbf{y}_j on the subgraph $\{\mathbf{y}_i, \mathbf{y}_j\} \cup \{\mathbf{y}_k : k > i, \mathbf{y}_k \text{ has at least one observed descendant}\}$. \square

Proof of Proposition 4. Note that for any set $g(i) \subset \{1, \dots, i-1\}$, we have $f(\mathbf{y}_i | \mathbf{y}_{g(i)}) = f(\mathbf{y}_i | \mathbf{y}_{g(i)}, \mathbf{z}_{g(i)})$, due to conditional independence between \mathbf{z}_k and any other variable in the model given \mathbf{y}_k . Thus, for latent Vecchia we can change the conditioning set $\mathbf{x}_{p(i)}$ from $\mathbf{y}_{q(i)}$ to $(\mathbf{y}_{q(i)}, \mathbf{z}_{q(i)})$ without changing the approximation. Likewise, for SGV we can change $\mathbf{x}_{p(i)}$ from $(\mathbf{y}_{q_y(i)}, \mathbf{z}_{q_z(i)})$ to $(\mathbf{y}_{q_y(i)}, \mathbf{z}_{q(i)})$ without changing the approximation since $q_y(i) \cup q_z(i) = q(i)$. Further, note that $\mathbf{z}_{q(i)}$ is contained in $(\mathbf{y}_{q_y(i)}, \mathbf{z}_{q(i)})$, which is contained in $(\mathbf{y}_{q(i)}, \mathbf{z}_{q(i)})$, and thus the proposition follows using Thm. 1 in Guinness (2016), which says that adding variables to the conditioning set in Vecchia approximations cannot increase the KL divergence from the true model. \square

Proof of Proposition 5. Without loss of generality, we assume that the locations lie on a regular unit-distance grid on the d -dimensional hypercube with $n_z^{1/d}$ unique values in each dimension, and we assume a lexicographic ordering in which locations are ordered first by their first coordinate, for those with same first coordinate by their second coordinate, and so forth. Let $\mathbf{s}_i = (s_{i1}, \dots, s_{id})$ be the location of \mathbf{y}_i (and \mathbf{z}_i). Consider a pair of locations \mathbf{s}_i and \mathbf{s}_j with $\mathbf{s}_j = (s_{i1} - t, s_{j2}, \dots, s_{jd})$, which under lexicographic ordering gives $j < i$ when $t > 0$. For $\mathbf{s}_a = (s_{i1} + 1, s_{j2}, \dots, s_{jd})$, we have $a > i$. Further, ignoring edge cases, we have $\mathbf{y}_j \rightarrow \mathbf{y}_a$ when $1 \leq t \leq t_m$, where $t_m = \mathcal{O}(m^{1/d})$, since the conditioning set of \mathbf{y}_a corresponds to the m locations roughly in a semi-ball around \mathbf{s}_a of radius t_m (e.g., $t_m = (2m/\pi)^{1/2}$ for $d = 2$). Also consider $\mathbf{s}_b = (s_{i1} + 1, s_{i2}, \dots, s_{id})$, for which also $b > i$. We can find a path between \mathbf{y}_a and \mathbf{y}_b on the subgraph $\{\mathbf{y}_k : k > i\}$, since all variables on the hyperplane $(s_{i1} + 1, \cdot, \dots, \cdot)$ are connected (if $m \geq d$) and have index greater than i . We also have $\mathbf{y}_i \rightarrow \mathbf{y}_b$. Therefore, there is a path from \mathbf{y}_j to \mathbf{y}_i on the subgraph $\{\mathbf{y}_j, \mathbf{y}_i\} \cup \{\mathbf{y}_k : k > i\}$, which by Proposition 3 means that \mathbf{V}_{ji} is non-zero. Since this is true for any $\mathbf{s}_j = \{s_{i1} - t, s_{j2}, \dots, s_{jd}\}$ with $1 \leq t \leq t_m$, there are $\mathcal{O}(n^{1-1/d} m^{1/d})$ nonzero elements in each of the n_z columns of \mathbf{V} , giving a memory complexity of $\mathcal{O}(n^{2-1/d} m^{1/d})$. As the time complexity for obtaining the reordered Cholesky factor \mathbf{V} is on the order of the sum of the squares of the number of nonzero elements per column in \mathbf{V} (e.g., Toledo, 2007, Thm. 2.2), the time complexity of obtaining \mathbf{V} from \mathbf{W} is $\mathcal{O}(n^{3-2/d} m^{2/d})$. \square

Proof of Proposition 6. First, we show that, for SGV, \mathbf{V} has at most mr off-diagonal elements per column. Using Proposition 3, that means that we need to show that, for any $j < i$, there is no path between \mathbf{y}_i and \mathbf{y}_j on the subgraph \mathcal{G}_{ij}^ℓ if $\mathbf{y}_j \not\rightarrow \mathbf{y}_i$, where $\mathcal{G}_{ij}^k := \{\mathbf{y}_i, \mathbf{y}_j\} \cup \{\mathbf{y}_t : \max(i, j) < t \leq k\}$. (Note that

this statement then also holds if we restrict the subgraph to vertices with observed descendants.) Define $D_i^k := \{t : \mathbf{y}_t \text{ is a descendant of } \mathbf{y}_i \text{ in } \mathcal{G}_{ij}^k\}$, and analogously for D_j^k . Thus, assuming that $\mathbf{y}_j \not\rightarrow \mathbf{y}_i$, we need to show that $D_i^k \cap D_j^k = \emptyset$, which we will do by induction. We have $\mathcal{G}_{ij}^{i+1} = \{\mathbf{y}_i, \mathbf{y}_j, \mathbf{y}_k\}$, where $q_y(k)$ can only contain either i or j by the rules of the SGV, because $j \notin q_y(i)$, and so $D_i^{i+1} \cap D_j^{i+1} = \emptyset$. Now, assume that $D_i^k \cap D_j^k = \emptyset$ for $k > i$. Then, for any $t_i \in D_i^k$ and $t_j \in D_j^k$, \mathbf{y}_{t_i} and \mathbf{y}_{t_j} cannot be adjacent. Hence, by the rules of the SGV, $q_y(k+1)$ can only contain either elements of D_i^k or of D_j^k , and so $D_i^{k+1} \cap D_j^{k+1} = \emptyset$. In summary, for the SGV and $j < i$, $\mathbf{V}_{ji} = \mathbf{0}$ unless $\mathbf{y}_j \rightarrow \mathbf{y}_i$, and so \mathbf{V} has at most mr off-diagonal elements per column.

The time complexity for obtaining the reordered Cholesky factor \mathbf{V} (and the selected inverse of \mathbf{W}) is on the order of the sum of the squares of the number of nonzero elements per column in \mathbf{V} (e.g., Toledo, 2007, Thm. 2.2). Hence, the time complexity for computing \mathbf{W} , its decomposition, and its selected inverse is $\mathcal{O}(nm^2r^2)$. The time and memory complexity for computing \mathbf{U} is $\mathcal{O}(nm^3r^2)$ and $\mathcal{O}(nmr)$ (i.e., at least as high as that for computing \mathbf{V}), and so SGV has the same computational complexity as standard Vecchia. \square

References

- Banerjee, S., Carlin, B. P., and Gelfand, A. E. (2004). *Hierarchical modeling and analysis for spatial data*. Chapman & Hall.
- Banerjee, S., Gelfand, A. E., Finley, A. O., and Sang, H. (2008). Gaussian predictive process models for large spatial data sets. *Journal of the Royal Statistical Society, Series B*, 70(4):825–848.
- Bevilacqua, M., Gaetan, C., Mateu, J., and Porcu, E. (2012). Estimating space and space-time covariance functions for large data sets: A weighted composite likelihood approach. *Journal of the American Statistical Association*, 107(497):268–280.
- Cressie, N. and Davidson, J. L. (1998). Image analysis with partially ordered Markov models. *Computational Statistics & Data Analysis*, 29(1):1–26.
- Cressie, N. and Johannesson, G. (2008). Fixed rank kriging for very large spatial data sets. *Journal of the Royal Statistical Society, Series B*, 70(1):209–226.
- Cressie, N. and Wikle, C. K. (2011). *Statistics for Spatio-Temporal Data*. Wiley, Hoboken, NJ.
- Datta, A., Banerjee, S., Finley, A. O., and Gelfand, A. E. (2016a). Hierarchical nearest-neighbor Gaussian process models for large geostatistical datasets. *Journal of the American Statistical Association*, 111(514):800–812.
- Datta, A., Banerjee, S., Finley, A. O., and Gelfand, A. E. (2016b). On nearest-neighbor Gaussian process models for massive spatial data. *Wiley Interdisciplinary Reviews: Computational Statistics*, 8(5):162–171.
- Datta, A., Banerjee, S., Finley, A. O., Hamm, N. A. S., and Schaap, M. (2016c). Non-separable dynamic nearest-neighbor Gaussian process models for large spatio-temporal data with an application to particulate matter analysis. *Annals of Applied Statistics*, 10(3):1286–1316.
- Eidsvik, J., Shaby, B. A., Reich, B. J., Wheeler, M., and Niemi, J. (2014). Estimation and prediction in spatial models with block composite likelihoods using parallel computing. *Journal of Computational and Graphical Statistics*, 23(2):295–315.
- Erismann, A. M. and Tinney, W. F. (1975). On computing certain elements of the inverse of a sparse matrix. *Communications of the ACM*, 18(3):177–179.
- Eubank, R. L. and Wang, S. J. (2002). The equivalence between the Cholesky decomposition and the Kalman filter. *The American Statistician*, 56(1):39–43.
- Finley, A. O., Datta, A., Cook, B. C., Morton, D. C., Andersen, H. E., and Banerjee, S. (2017). Applying nearest neighbor Gaussian processes to massive spatial data sets: Forest canopy height prediction across Tanana Valley Alaska. *arXiv:1702.00434*.
- Finley, A. O., Sang, H., Banerjee, S., and Gelfand, A. E. (2009). Improving the performance of predictive process modeling for large datasets. *Computational Statistics & Data Analysis*, 53(8):2873–2884.
- Furrer, R., Genton, M. G., and Nychka, D. (2006). Covariance tapering for interpolation of large spatial datasets. *Journal of Computational and Graphical Statistics*, 15(3):502–523.

- Furrer, R. and Sain, S. R. (2010). spam: A sparse matrix R package with emphasis on MCMC methods for Gaussian Markov random fields. *Journal of Statistical Software*, 36(10):1–25.
- Gramacy, R. B. and Apley, D. W. (2015). Local Gaussian process approximation for large computer experiments. *Journal of Computational and Graphical Statistics*, 24(2):561–578.
- Gramacy, R. B. and Lee, H. K. (2012). Cases for the nugget in modeling computer experiments. *Statistics and Computing*, 22(3):713–722.
- Guinness, J. (2016). Permutation methods for sharpening Gaussian process approximations. *arXiv:1609.05372*.
- Higdon, D. (1998). A process-convolution approach to modelling temperatures in the North Atlantic Ocean. *Environmental and Ecological Statistics*, 5(2):173–190.
- Huang, H. and Sun, Y. (2016). Hierarchical low rank approximation of likelihoods for large spatial datasets. *arXiv:1605.08898*.
- Kalman, R. (1960). A new approach to linear filtering and prediction problems. *Journal of Basic Engineering*, 82(1):35–45.
- Katzfuss, M. (2017). A multi-resolution approximation for massive spatial datasets. *Journal of the American Statistical Association*, 112(517):201–214.
- Katzfuss, M. and Cressie, N. (2011). Spatio-temporal smoothing and EM estimation for massive remote-sensing data sets. *Journal of Time Series Analysis*, 32(4):430–446.
- Kaufman, C. G., Schervish, M. J., and Nychka, D. W. (2008). Covariance tapering for likelihood-based estimation in large spatial data sets. *Journal of the American Statistical Association*, 103(484):1545–1555.
- Lauritzen, S. L. (1996). *Graphical Models*. Clarendon Press.
- Li, S., Ahmed, S., Klimeck, G., and Darve, E. (2008). Computing entries of the inverse of a sparse matrix using the FIND algorithm. *Journal of Computational Physics*, 227(22):9408–9427.
- Lin, L., Yang, C., Meza, J., Lu, J., Ying, L., and Weinan, E. (2011). SelInv - An algorithm for selected inversion of a sparse symmetric matrix. *ACM Transactions on Mathematical Software*, 37(4):40.
- Lindgren, F., Rue, H., and Lindström, J. (2011). An explicit link between gaussian fields and gaussian markov random fields: the stochastic partial differential equation approach. *Journal of the Royal Statistical Society: Series B*, 73(4):423–498.
- Nychka, D. W., Bandyopadhyay, S., Hammerling, D., Lindgren, F., and Sain, S. R. (2015). A multi-resolution Gaussian process model for the analysis of large spatial data sets. *Journal of Computational and Graphical Statistics*, 24(2):579–599.
- OCO-2 Science Team, Gunson, M., and Eldering, A. (2015). OCO-2 Level 2 bias-corrected solar-induced fluorescence and other select fields from the IMAP-DOAS algorithm aggregated as daily files, retrospective processing V7r. https://disc.gsfc.nasa.gov/datacollection/OCO2.L2.Lite.SIF_7r.html.
- Quiñonero-Candela, J. and Rasmussen, C. E. (2005). A unifying view of sparse approximate Gaussian process regression. *Journal of Machine Learning Research*, 6:1939–1959.
- Rasmussen, C. E. and Williams, C. K. I. (2006). *Gaussian Processes for Machine Learning*. MIT Press.
- Rauch, H., Rauch, H., Tung, F., and Striebel, C. (1965). Maximum likelihood estimates of linear dynamic systems. *AIAA Journal*, 3(8):1445–1450.
- Rue, H. and Held, L. (2005). *Gaussian Markov Random Fields: Theory and Applications*. CRC press.
- Rue, H. and Held, L. (2010). Discrete spatial variation. In *Handbook of Spatial Statistics*, chapter 12, pages 171–200. CRC Press.
- Rütimann, P. and Bühlmann, P. (2009). High dimensional sparse covariance estimation via directed acyclic graphs. *Electronic Journal of Statistics*, 3:1133–1160.
- Sang, H. and Huang, J. Z. (2012). A full scale approximation of covariance functions. *Journal of the Royal Statistical Society, Series B*, 74(1):111–132.
- Sang, H., Jun, M., and Huang, J. Z. (2011). Covariance approximation for large multivariate spatial datasets with an application to multiple climate model errors. *Annals of Applied Statistics*, 5(4):2519–2548.
- Snelson, E. and Ghahramani, Z. (2007). Local and global sparse Gaussian process approximations. In

Artificial Intelligence and Statistics 11 (AISTATS).

- Stein, M. L. (2011). When does the screening effect hold? *The Annals of Statistics*, 39(6):2795–2819.
- Stein, M. L. (2014). Limitations on low rank approximations for covariance matrices of spatial data. *Spatial Statistics*, 8:1–19.
- Stein, M. L., Chi, Z., and Welty, L. (2004). Approximating likelihoods for large spatial data sets. *Journal of the Royal Statistical Society: Series B*, 66(2):275–296.
- Sun, Y. and Stein, M. L. (2016). Statistically and computationally efficient estimating equations for large spatial datasets. *Journal of Computational and Graphical Statistics*, 25(1):187–208.
- Toledo, S. (2007). Lecture Notes on Combinatorial Preconditioners, Chapter 3. <http://www.tau.ac.il/~stoledo/Support/chapter-direct.pdf>.
- Vecchia, A. (1988). Estimation and model identification for continuous spatial processes. *Journal of the Royal Statistical Society, Series B*, 50(2):297–312.
- Wikle, C. K. and Cressie, N. (1999). A dimension-reduced approach to space-time Kalman filtering. *Biometrika*, 86(4):815–829.